

Two-dimensional Langevin modeling of fission dynamics of the excited compound nuclei ^{188}Pt , ^{227}Pa and ^{251}Es

H. Eslamizadeh¹⁾

Department of Physics, Persian Gulf University 7516913817, Bushehr, Iran

Abstract: A stochastic approach based on one- and two-dimensional Langevin equations is applied to calculate the pre-scission neutron multiplicity, fission probability, anisotropy of fission fragment angular distribution, fission cross section and the evaporation cross section for the compound nuclei ^{188}Pt , ^{227}Pa and ^{251}Es in an intermediate range of excitation energies. The chaos weighted wall and window friction formula are used in the Langevin equations. The elongation parameter, c , is used as the first dimension and projection of the total spin of the compound nucleus onto the symmetry axis, K , considered as the second dimension in Langevin dynamical calculations. A constant dissipation coefficient of K , $\gamma_K = 0.077(\text{MeV zs})^{-1/2}$, is used in two-dimensional calculations to reproduce the above mentioned experimental data. Comparison of the theoretical results of the pre-scission neutron multiplicity, fission probability, fission cross section and the evaporation cross section with the experimental data shows that the results of two-dimensional calculations are in better agreement with the experimental data. Furthermore, it is shown that the two-dimensional Langevin equations together with a dissipation coefficient of K , $\gamma_K = 0.077(\text{MeV zs})^{-1/2}$, can satisfactorily reproduce the anisotropy of fission fragment angular distribution for the heavy compound nucleus ^{251}Es . However, a larger value of $\gamma_K = 0.250(\text{MeV zs})^{-1/2}$ is needed to reproduce the anisotropy of fission fragment angular distribution for the lighter compound nucleus ^{227}Pa .

Keywords: Langevin fission dynamics, mean neutron multiplicity, nuclear viscosity

PACS: 25.70.Jj, 24.75.+i **DOI:** 10.1088/1674-1137/40/2/024103

1 Introduction

During recent decades different dynamical and statistical models have been extensively and rather successfully used to elucidate many problems of fusion–fission reactions (see, for example Refs. [1-20]). Many researchers in their computational representations of different features of fusion–fission reactions have assumed that compound nuclei have zero spin about the symmetry axis. This assumption is not consistent with either the statistical model or with a dynamical treatment of the orientation degree of freedom, the K coordinate, as first pointed out by Lestone in Ref. [21]. The authors in Ref. [10] also stressed that a large volume of heavy-ion-induced fission data needs to be reanalyzed using a dynamical treatment of the orientation degree of freedom. Consequently, in the present study we consider the dynamical evolution of the orientation degree of freedom K to calculate the pre-scission neutron multiplicity, fission probability, anisotropy of fission fragment angular distribution, fission cross section and the evaporation cross section for the compound nuclei ^{188}Pt , ^{227}Pa

and ^{251}Es . Furthermore, in our calculations, we consider the deformation effects on determination of the particle binding energies [22] to accurately reproduce the above mentioned experimental data.

The present paper has been arranged as follows. In Section 2, we describe the model and basic equations. The results of calculations are presented in Section 3. Finally, concluding remarks are given in Section 4.

2 Details of the model

In the present investigation, we use the well-known $\{c, h, \alpha\}$ parameterization [23] to describe the nuclear shapes. This parameterization was successfully used both in statistical calculations and in dynamical calculations. However, we simplify the calculation by considering only symmetric fission ($\alpha = 0$) and further ignore the neck degree of freedom ($h = 0$). In cylindrical coordinates the surface of a nucleus of mass number A can be defined as

$$\rho^2(z) = (1 - z^2/c_0^2)(a_0c_0^2 + b_0z^2), \quad (1)$$

Received 7 July 2015

1) E-mail: m.eslamizadeh@yahoo.com

©2016 Chinese Physical Society and the Institute of High Energy Physics of the Chinese Academy of Sciences and the Institute of Modern Physics of the Chinese Academy of Sciences and IOP Publishing Ltd

where

$$\begin{cases} c_0 = cR, R = 1.16A^{1/3} \\ a_0 = 1/c^3 - b_0/5, b_0 = (c-1)/2, \end{cases} \quad (2)$$

where z is the coordinate along the symmetry axis and ρ is the radial coordinate. The Langevin equations in one dimension can be expressed as

$$\begin{aligned} \frac{dp}{dt} &= -\frac{p^2}{2} \frac{\partial}{\partial c} \left(\frac{1}{m} \right) - \frac{\partial F}{\partial c} - \eta \dot{c} + R(t), \\ \frac{dc}{dt} &= \frac{p}{m(c)}, \end{aligned} \quad (3)$$

where c is the elongation parameter and p is the conjugate momentum. m and η are the shape-dependent collective inertia and friction coefficients, respectively. $R(t)$ is a random force with the properties $\langle R(t) \rangle = 0$ and $\langle R(t)R(t') \rangle = 2\eta T \delta(t-t')$, and F is the free energy of the system

$$F(c, T) = V(c) - a(c)T^2, \quad (4)$$

where $V(c)$ and T are the potential energy and temperature of the system, respectively. The coordinate-dependent level density parameter $a(c)$ can be considered as follows

$$a(c) = a_v A + a_s A^{2/3} B_s(c), \quad (5)$$

where A is the mass number of the compound nucleus, and B_s is the dimensionless functional of the surface energy in the liquid drop model. The values of the parameters $a_v = 0.073 \text{ MeV}^{-1}$ and $a_s = 0.095 \text{ MeV}^{-1}$ in Eq. (5) are taken from the work of Ignatyuk et al. [24]. The collective inertia, m , is obtained by assuming an incompressible irrotational flow and making the Werner-Wheeler approximation [25]. The potential energy can be obtained from the liquid drop model with a finite range of nuclear forces as Refs. [10, 26]

$$\begin{aligned} V(c, A, Z, I, K, T) &= (S'(c) - 1)E_s^0(A, Z) \\ &+ (C(c) - 1)0.7053 \frac{Z^2}{A^{1/3}} + \frac{(I(I+1) - K^2)\hbar^2}{I_{\perp}(c) \frac{4}{5} M R_0^2 + 8M a^2} \\ &+ \frac{K^2 \hbar^2}{I_{\parallel}(c) \frac{4}{5} M R_0^2 + 8M a^2}, \end{aligned} \quad (6)$$

where E_c^0 and E_s^0 are the Coulomb and surface energies of the corresponding spherical system and can be determined as Refs. [27, 28]. $C(c)$, $I_{\perp}(c)$ and $I_{\parallel}(c)$ are the Coulomb energy and moments of inertia perpendicular to and about the symmetry axis for a sharp-edged nuclear density distribution. M and R_0 are the mass and radius of the spherical system. $S'(c)$ is an empirically adjusted surface energy in units of the corresponding spherical value [26] and $a = 0.6 \text{ fm}$. Figure 1 shows the potential energy surface calculated with Eq. (6) for the

compound nucleus ^{227}Pa in the collective coordinates c and K at $I = 30\hbar$. It can be seen from Fig. 1 that the inclusion of the K coordinate changes the fission barrier height. It is also clear from Fig. 1 that the height of the potential energy surface increases with increasing K .

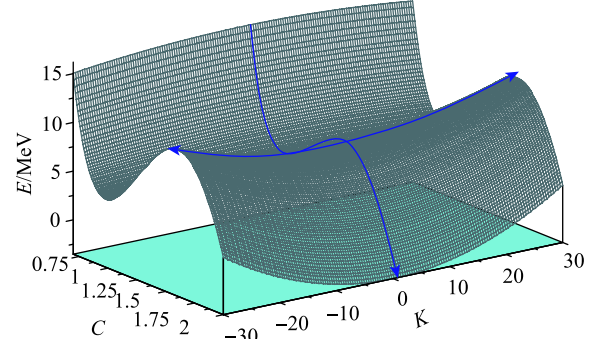


Fig. 1. (color online) The potential energy surface for the compound nucleus ^{227}Pa in the collective coordinates c and K at $I = 30\hbar$.

In our calculations, we should specify the entrance channel through which a compound nucleus is formed. Assuming complete fusion of the projectile with the target, the spin distribution of the compound nucleus can be described by the formula

$$\frac{d\sigma(I)}{dI} = \frac{2\pi}{k^2} \frac{2I+1}{1 + \exp\left(\frac{I-I_c}{\delta I}\right)}, \quad (7)$$

where I_c is the critical spin and δI is the diffuseness. The parameters I_c and δI can be approximated by the relations presented in Ref. [13]. The initial spin of the compound nucleus can be obtained by sampling the above spin distribution function.

In the present calculations, dissipation is generated through the chaos weighted wall and window friction formula. For small elongation before neck formation we use the chaos weighted wall formula, and after neck formation we use the chaos weighted wall and window friction formula

$$\eta(c) = \begin{cases} \mu(c)\eta_{\text{wall}}(c) & \text{for } c < c_{\text{win}} \\ \mu(c)\eta_{\text{wall}}(c) + \eta_{\text{win}}(c) & \text{for } c \geq c_{\text{win}}. \end{cases} \quad (8)$$

The magnitude of chaoticity μ changes from 0 to 1 as the nucleus evolves from a spherical to a deformed shape. The chaoticity μ is a measure of chaos in the single particle motion and depends on the shape of the nucleus. In the classical picture this can be given as the average fraction of the nucleon trajectories which are chaotic and is evaluated by sampling over a large number of classical trajectories for a given shape of the nucleus. Each such trajectory is identified either as a regular or a chaotic

one by considering the magnitude of its Lyapunov exponent and the nature of its variation with time [29]. η_{wall} and η_{win} can be calculated as Refs. [30–32]. For nuclear shapes featuring no neck ($c < c_{\text{win}}$)

$$\eta_{\text{wall}}(c) = \frac{\pi\rho_m}{2}\bar{v} \int_{z_{\text{min}}}^{z_{\text{max}}} \left(\frac{\partial\rho^2}{\partial c}\right)^2 \left[\rho^2 + \left(\frac{1}{2}\frac{\partial\rho^2}{\partial z}\right)^2\right]^{-1/2} dz, \quad (9)$$

and for nuclear shapes featuring a neck ($c \geq c_{\text{win}}$)

$$\begin{aligned} \eta_{\text{wall}}(c) &= \frac{\pi\rho_m}{2}\bar{v} \left\{ \int_{z_{\text{min}}}^{z_N} \left(\frac{\partial\rho^2}{\partial c} + \frac{\partial\rho^2}{\partial z} \frac{\partial D_1}{\partial c}\right)^2 \right. \\ &\times \left[\rho^2 + \left(\frac{1}{2}\frac{\partial\rho^2}{\partial z}\right)^2\right]^{-1/2} dz + \int_{z_N}^{z_{\text{max}}} \left(\frac{\partial\rho^2}{\partial c} + \frac{\partial\rho^2}{\partial z} \frac{\partial D_2}{\partial c}\right)^2 \\ &\times \left[\rho^2 + \left(\frac{1}{2}\frac{\partial\rho^2}{\partial z}\right)^2\right]^{-1/2} dz \left. \right\}, \quad (10) \end{aligned}$$

$$\eta_{\text{win}}(c) = \frac{1}{2}\rho_m\bar{v} \left(\frac{\partial R}{\partial c}\right)^2 \Delta\sigma, \quad (11)$$

where ρ_m is the mass density of the nucleus, \bar{v} is the average nucleon speed inside the nucleus, D_1, D_2 are positions of mass centers of the two parts of the fissioning system relative to the center of mass of the whole system, ρ is the radial coordinate of the nuclear surface, $\Delta\sigma$ is an area of the window between two parts of the system, R is the distance between centers of mass of future fragment, z_N is the position of the neck plane that divides the nucleus into two parts, and z_{min} and z_{max} are the left and right ends of the nuclear shape.

In our calculations, we start modeling fission dynamics from the ground state with the excitation energy E^* of the compound nucleus. Evaporation of pre-scission light particles along a Langevin trajectory is taken into account using a Monte Carlo simulation technique. The decay widths for emission n, p, α and γ quanta are calculated at each Langevin time step Δt . The emission of a particle is allowed by asking at each time step along the trajectory whether the ratio of the Langevin time step Δt to the particle decay time τ_{part} is larger than a random number ξ

$$\Delta t / \tau_{\text{part}} > \xi \quad (0 \leq \xi \leq 1), \quad (12)$$

where $\tau_{\text{part}} = \hbar / \Gamma_{\text{tot}}$ and $\Gamma_{\text{tot}} = \sum_{\nu} \Gamma_{\nu}$, ($\nu = n, p, \alpha, \gamma$).

The probabilities of decay via different channels can be calculated using a standard Monte Carlo cascade procedure where the kind of decay is selected with the weights $\Gamma_{\nu} / \Gamma_{\text{tot}}$. After the particle type is randomly chosen, the kinetic energy ε_{ν} of the emitted particle is also generated via a Monte Carlo procedure. The intrinsic excitation

energy, mass, and spin of the residual compound nucleus are recalculated and the dynamics is continued. The loss of angular momentum is taken into account by assuming that each neutron, proton, or γ quantum carries away $1\hbar$ while the α particle carries away $2\hbar$. In the simulation of evolution of a fissile nucleus a Langevin trajectory either reaches the scission point, in which case it is counted as a fission event, or if the excitation energy for a trajectory which is still inside the saddle reaches the value $E_{\text{int}} + E_{\text{coll}} < \min(B_{\nu}, B_f)$, the event is counted as an evaporation residue (B_{ν} is the binding energy of the particle $\nu = n, p, \alpha, \gamma$ and B_f is the fission barrier height).

The particle emission width of a particle of kind ν can be calculated as in Ref. [33]:

$$\begin{aligned} \Gamma_{\nu} &= (2s_{\nu} + 1) \frac{m_{\nu}}{\pi^2 \hbar^2 \rho_c(E_{\text{int}})} \\ &\times \int_0^{E_{\text{int}} - B_{\nu}} d\varepsilon_{\nu} \rho_R(E_{\text{int}} - B_{\nu} - \varepsilon_{\nu}) \varepsilon_{\nu} \sigma_{\text{inv}}(\varepsilon_{\nu}), \quad (13) \end{aligned}$$

where $\rho_c(E_{\text{int}})$ and $\rho_R(E_{\text{int}} - B_{\nu} - \varepsilon_{\nu})$ are the level densities of the compound and residual nuclei, s_{ν} is the spin of the emitted particle ν , and m_{ν} is its reduced mass with respect to the residual nucleus. The intrinsic energy and the separation energy of particle ν are denoted by E_{int} and B_{ν} . The variable ε_{ν} is the kinetic energy of the evaporated particle ν . The inverse cross sections can be written as [33]:

$$\sigma_{\text{inv}}(\varepsilon_{\nu}) = \begin{cases} \pi R_{\nu}^2 (1 - V_{\nu} / \varepsilon_{\nu}) & \text{for } \varepsilon_{\nu} > V_{\nu} \\ 0 & \text{for } \varepsilon_{\nu} < V_{\nu} \end{cases}, \quad (14)$$

with

$$R_{\nu} = 1.21 [(A - A_{\nu})^{1/3} + A_{\nu}^{1/3}] + (3.4 / \varepsilon_{\nu}^{1/2}) \delta_{\nu, n}, \quad (15)$$

where A_{ν} is the mass number of the emitted particle $\nu = n, p, \alpha$. The barriers for the charged particles are

$$V_{\nu} = [(Z - Z_{\nu}) Z_{\nu} K_{\nu}] / (R_{\nu} + 1.6), \quad (16)$$

with $K_{\nu} = 1.15$ for proton and 1.32 for α .

The width of the gamma emission can be calculated as in Ref. [34].

The conservation of energy is satisfied by

$$E^* = E_{\text{int}}(t) + E_{\text{coll}} + V(c, I, K) + E_{\text{evap}}(t), \quad (17)$$

where E^* is the total excitation energy of the nucleus, E_{coll} and $E_{\text{evap}}(t)$ are the kinetic energy of the collective motion of the nucleus and energy carried away by evaporated particles, respectively. The variation of the orientation degree of freedom (K coordinate) can be determined by using the following equation [10]

$$dK = -\frac{\gamma_K^2 I^2}{2} \frac{\partial V}{\partial K} dt + \gamma_K I \sqrt{T} d\xi(t), \quad (18)$$

where γ_K is a parameter controlling the coupling between the orientation degree of freedom K and the heat bath and $\xi(t)$ is a random variable that possesses the following statistical properties $\langle \xi_i \rangle = 0$ and $\langle \xi_i(t_1)\xi_j(t_2) \rangle = 2\delta_{ij}\delta(t_1 - t_2)$. By averaging Eq. (18), it can be shown that

$$\frac{d\langle K \rangle}{dt} = -\frac{\gamma_K^2 I^2}{2} \left\langle \frac{\partial V}{\partial K} \right\rangle. \quad (19)$$

From the expression for the rotational energy (the last two terms in Eq. (6)), it follows that

$$\frac{d\langle K \rangle}{dt} = -\frac{\gamma_K^2 I^2 \hbar^2}{2J_{\text{eff}}} \langle K \rangle. \quad (20)$$

Assuming a constant γ_K , it can be shown that the solution of this equation has the form

$$\langle K(t) \rangle_{K_0} = K_0 \exp \left[-\frac{\gamma_K^2 I^2 \hbar^2}{2J_{\text{eff}}} (t - t_0) \right], \quad (21)$$

which gives the following expression for the relaxation time as

$$\tau_K = \frac{2J_{\text{eff}}}{\gamma_K^2 I^2 \hbar^2}. \quad (22)$$

The authors in Refs. [10, 35], based on the works of Døssing and Randrup [36, 37], have shown that the dissipation coefficient of K can be calculated as

$$\gamma_K(c) = \frac{1}{RR_N \sqrt{2\pi^3 n_0}} \sqrt{\frac{J_R |J_{\text{eff}}| J_{\parallel}}{J_{\perp}^3}}, \quad (23)$$

where R_N is the neck radius, R is the distance between the centers of mass of the nascent fragment, $n_0 = 0.0263$ MeV zs fm⁻⁴ is the bulk flux in the standard nuclear matter [36] and $J_R = MR^2/4$ for a reflection symmetric shape. It should be noted that the Langevin equation for the K coordinate, Eq. (18), and the Langevin equations, Eq. (3), are connected through the potential energy. The Langevin dynamics of the K coordinate depends on the value of the potential energy. At the same time, the rotational part of the potential energy is dependent on the value of K at time t . Consequently, in this way K coordinate can affect the dynamical evolution of the shape variable.

The fission cross section can be obtained in terms of the fusion cross section as follows

$$\sigma_{\text{fiss}} = \sum_I \sigma_{\text{fus}}(I) \frac{\Gamma_f}{\Gamma_{\text{tot}}}. \quad (24)$$

In the present paper, we use the saddle point transition model (SPTS) [38–40] to analyze the fission fragment angular distributions. In analyzing the fission fragment angular distributions, it is usually assumed that fission fragment travel in the direction of the symmetry axis of the nucleus. Consequently, the fission fragment angular

distributions can be determined by three quantum numbers: I, M, K , where I is the spin of a compound nucleus, M is the projection of I on the axis of the projectile ion beam, and K is the projection of I on the symmetry axis of the nucleus. In the case of heavy-ion-induced fission reactions, the spin of the compound nucleus is usually much larger than the ground state spins of the target and projectile, and is perpendicular to the beam axis, so that $M = 0$. At fixed values of I and K , the angular distribution can be determined as follows

$$W(\theta, I, K) = (I + 1/2) |d_{M=0, K}^I(\theta)|^2, \quad (25)$$

where θ is the angle between the beam axis and the nuclear symmetry axis and function $d_{M, K}^I(\theta)$ can be defined as in Ref. [38]. At high values of I , $W(\theta, I, K)$ can be approximated as

$$W(\theta, I, K) \approx \frac{I + 1/2}{\pi} \times [(I + 1/2)^2 \sin^2 \theta - K^2]^{1/2}. \quad (26)$$

The fission fragment angular distribution can be calculated by averaging Eq. (25) over the quantum numbers I and K as follows

$$W(\theta) = \sum_{I=0}^{\infty} \sigma_I \sum_{K=-I}^I P(K) W(\theta, I, K). \quad (27)$$

It is clear from Eq. (27) that for calculation of the angular distribution, it is necessary to specify the type of distributions σ_I and $P(K)$ of the compound nuclei over I and K , respectively. In the SPTS model an equilibrium distribution of K values is assumed, this is determined by the Boltzmann factor $\exp(-E_{\text{rot}}/T)$ [40] at the saddle point. Therefore, the equilibrium distribution with respect to K can be expressed as

$$P_{\text{eq}}(K) = \frac{\exp(-K^2/(2K_0^2))}{\sum_{K=-I}^I \exp(-K^2/(2K_0^2))}, \quad (28)$$

where variance of the equilibrium K distribution, K_0 , is given by the expression $K_0^2 = (T/\hbar^2)I_{\text{eff}}$ and $I_{\text{eff}} = I_{\parallel}I_{\perp}/(I_{\perp} - I_{\parallel})$, where I_{\parallel}, I_{\perp} , are the parallel and perpendicular moments of inertia which are calculated at the transition state and T is the nuclear temperature. It can be shown that the anisotropy of fission fragment angular distribution can be given by the approximate relation

$$A = \frac{\langle W(180^\circ) \rangle}{\langle W(90^\circ) \rangle} \approx 1 + \frac{\langle I^2 \rangle}{4K_0^2}. \quad (29)$$

3 Results and discussion

In the present investigation, we have used a stochastic approach based on one- and two-dimensional Langevin equations to calculate the pre-scission neutron multiplicity, fission probability, anisotropy of fission fragment angular distribution, fission cross section and the evaporation cross section for the compound nuclei ^{188}Pt , ^{227}Pa and ^{251}Es produced in the reactions $^{19}\text{F}+^{169}\text{Tm}$, $^{19}\text{F}+^{208}\text{Pb}$ and $^{19}\text{F}+^{232}\text{Th}$, respectively. In the one-dimensional calculations we have used only the elongation parameter c and in the two-dimensional calculations, we have used the elongation parameter c and the projection of the total spin of the compound nucleus onto the symmetry axis. Furthermore, in our dynamical calculations, we have used a constant dissipation coefficient of K , $\gamma_K = 0.077(\text{MeV zs})^{-1/2}$ to simulate the dynamics of nuclear fission of the compound nuclei ^{188}Pt , ^{227}Pa and ^{251}Es . It should be stressed that the authors in Ref. [41] obtained the value of $0.077(\text{MeV zs})^{-1/2}$ for the dissipation coefficient of K . Figures 2 and 3 show the results of pre-scission neutron multiplicity and fission probability

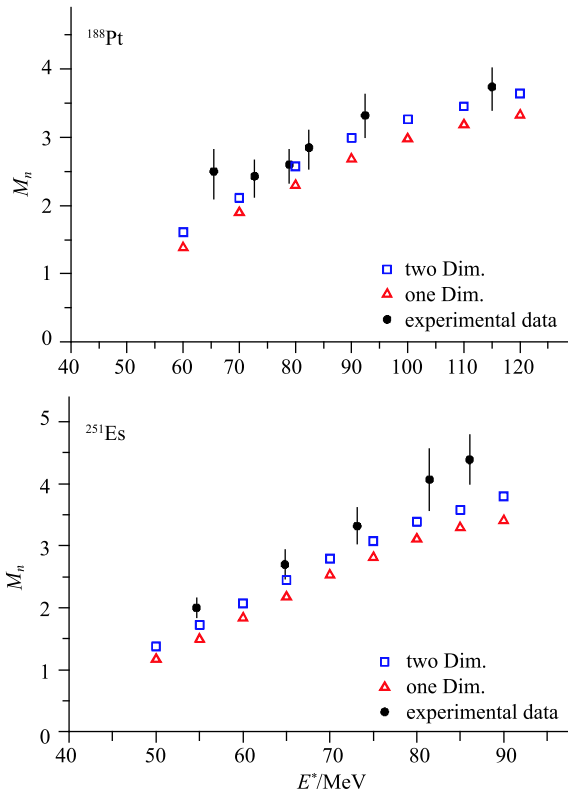


Fig. 2. (color online) Pre-scission neutron multiplicities for the compound nuclei ^{188}Pt and ^{251}Es as a function of excitation energy. The open triangles and open squares are the calculated results with one- and two-dimensional Langevin equations, respectively. The closed circles are the experimental data [42, 43].

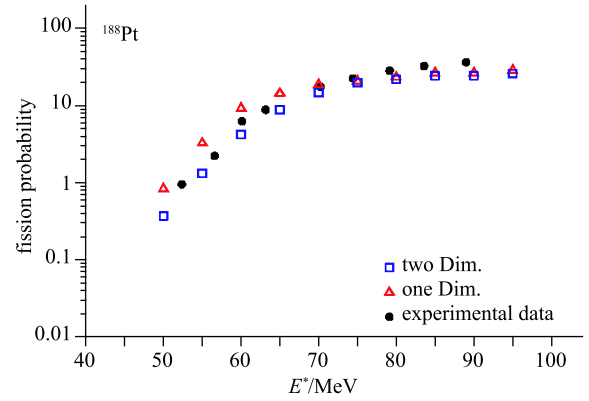


Fig. 3. (color online) Fission probability as a function of excitation energy for the compound nucleus ^{188}Pt . The open triangles and open squares are the calculated results with one- and two-dimensional Langevin equations, respectively. The closed circles are the experimental data [44].

calculated for the compound nuclei ^{188}Pt and ^{251}Es . It is clear from Figs. 2 and 3 that the results of the two-dimensional calculations can reproduce the experimental data more accurately than the one-dimensional calculations.

It can be seen from Fig. 2 that the two-dimensional calculations predict a larger pre-scission neutron multiplicity than the one-dimensional calculations. This can be explained as follows: the fission barrier height increases when considering the effect of the K coordinate in calculation of the potential energy (see Fig. 1). Such an increase of fission barrier height decreases the fission rate and increases the fission time and consequently increases the number of evaporated pre-scission particles.

It can also be seen from Fig. 3 that at higher excitation energies the fission probability reaches a stationary value. This is because with increasing excitation energy the pre-scission particle multiplicity increases and each emission of a light particle carries away excitation energy and angular momentum, therefore the fission barrier height of the residual nucleus increases and consequently the fission event is less and less probable.

In our calculations, in order to distinguish only the effect of the K coordinate on the fission rate, we have performed the calculations with fixed spin $I = 30\hbar$ and without taking into account the evaporation of pre-scission particles. In Fig. 4, we have demonstrated the influence of the K coordinate on the fission rate of the compound nucleus ^{188}Pt at fixed spin $I = 30\hbar$ and $E^* = 80$ MeV. It is clear from Fig. 4 that the fission rate decreases when considering the effect of the K coordinate in two-dimensional calculations.

In the present investigation, we have also calculated the fission and evaporation cross sections for the compound nucleus ^{188}Pt as a function of excitation energy.

The results of the calculations are presented in Figs. 5 and 6. It can be seen from Figs. 5 and 6 that the results of the two-dimensional calculations can reproduce the experimental data more accurately.

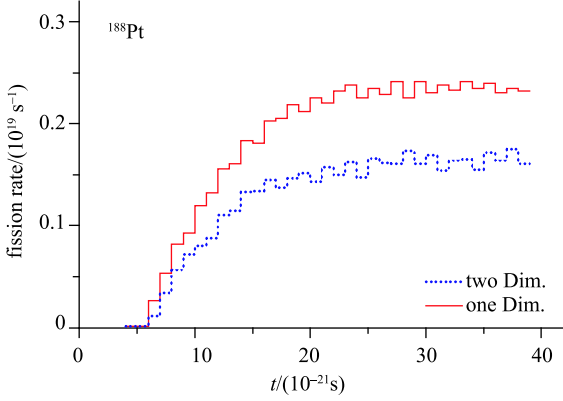


Fig. 4. (color online) The results of fission rate for the compound nucleus ^{188}Pt as a function of time at fixed spin $I = 30\hbar$ and $E^* = 80$ MeV. The solid and dotted curves are the calculated results with one- and two-dimensional Langevin equations, respectively.

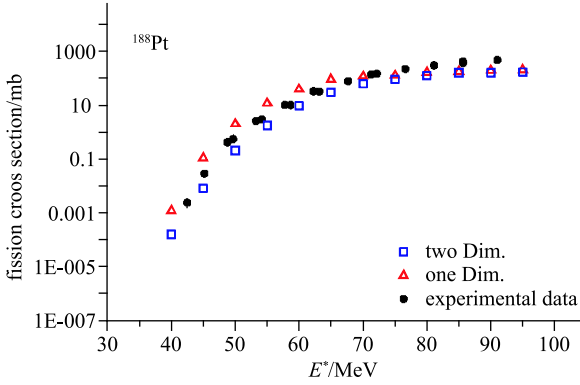


Fig. 5. (color online) Results of fission cross section for the compound nucleus ^{188}Pt as a function of excitation energy. The open triangles and open squares are the calculated results with one- and two-dimensional Langevin equations, respectively. The experimental data (closed circles) are taken from Ref. [44].

Finally, we have calculated the anisotropy of the fission fragment angular distribution for the compound nuclei ^{227}Pa and ^{251}Es . Figure 7 shows the calculated results of anisotropy of the fission fragment angular distribution for the compound nuclei ^{227}Pa and ^{251}Es . The open triangles and open squares in Fig. 7 are the calculated results of one- and two-dimensional Langevin equations together with $\gamma_K = 0.077(\text{MeV zs})^{-1/2}$ respectively, and the open circles are the results of the two-dimensional Langevin equations together with $\gamma_K = 0.250(\text{MeV zs})^{-1/2}$.

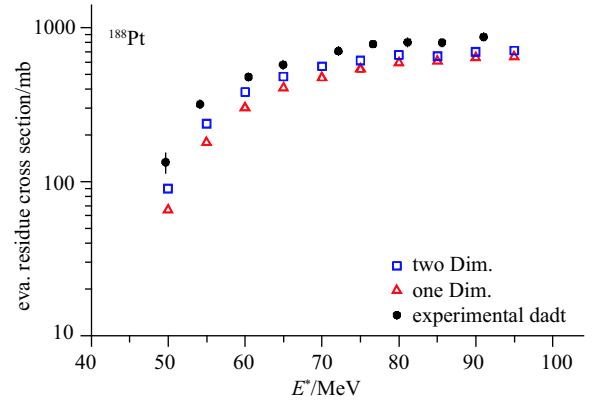


Fig. 6. (color online) Results of evaporation residue cross section for the compound nucleus ^{188}Pt as a function of excitation energy. The open triangles and open squares are the calculated results with one- and two-dimensional Langevin equations, respectively. The experimental data (closed circles) are taken from Ref. [44].

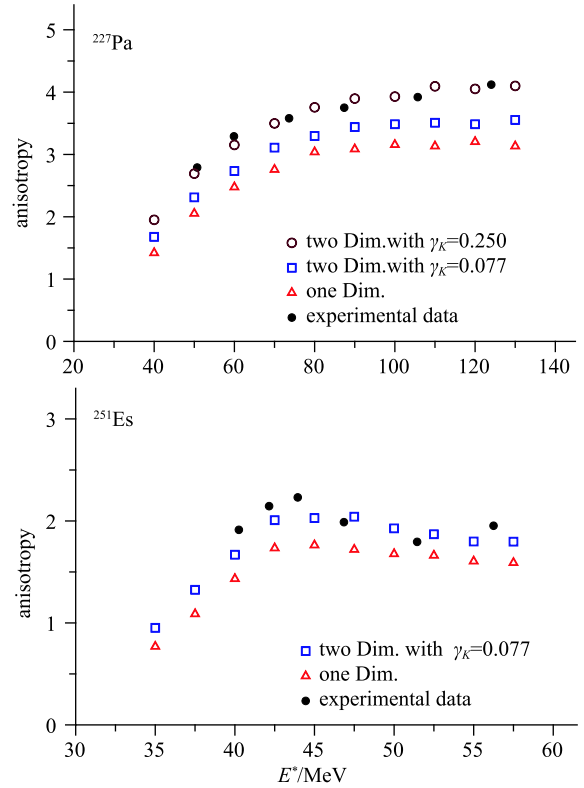


Fig. 7. (color online) Anisotropy of fission fragment angular distribution for the compound nuclei ^{227}Pa and ^{251}Es as a function of excitation energy. The experimental data (closed circles) are taken from Refs. [45, 46].

It can be seen from Fig. 7 that the results of the two-dimensional calculations together with a dissipation coefficient of K , $\gamma_K = 0.077(\text{MeV zs})^{-1/2}$, can satisfactorily reproduce the anisotropy of fission fragment angular

distribution for the heavy compound nucleus ^{251}Es . However, a larger value of $\gamma_K = 0.250(\text{MeV zs})^{-1/2}$ is needed to reproduce the anisotropy of fission fragment angular distribution for the lighter compound nucleus ^{227}Pa . This can be explained by considering Eq. (22) for the relaxation time of the K collective coordinate. The larger γ_K value causes a faster relaxation of the K coordinate and more narrow K distribution, which corresponds to the large A values as can be seen from Eq. (29).

4 Conclusions

A stochastic approach based on one- and two-dimensional Langevin equations has been applied to reproduce the experimental data on the pre-scission neutron multiplicity, fission probability, anisotropy of fission fragment angular distribution, fission cross section and the evaporation cross section for the compound nuclei ^{188}Pt , ^{227}Pa and ^{251}Es . The chaos weighted wall and window friction formula has been used in the Langevin equations. In the two-dimensional calculations, a constant

dissipation coefficient of K , $\gamma_K = 0.077(\text{MeV zs})^{-1/2}$ has been used to reproduce the above mentioned experimental data. Comparison of the theoretical results of the pre-scission neutron multiplicity, fission probability, fission cross section and the evaporation cross section with the experimental data showed that the results of the two-dimensional calculations are in better agreement with the experimental data. Furthermore, one- and two-dimensional Langevin equations have been used to calculate the anisotropy of fission fragment angular distribution for the compound nuclei ^{227}Pa and ^{251}Es . It was shown that the two-dimensional Langevin equations together with a dissipation coefficient of K , $\gamma_K = 0.077(\text{MeV zs})^{-1/2}$ can satisfactorily reproduce the anisotropy of fission fragment angular distribution for the heavy compound nucleus ^{251}Es . However, a larger value of $\gamma_K = 0.250(\text{MeV zs})^{-1/2}$ is needed to reproduce the anisotropy of fission fragment angular distribution for the compound nucleus ^{227}Pa .

The support of the Research Committee of the Persian Gulf University is greatly acknowledged.

References

- 1 P. N. Nadtochy et al, Phys. Rev. C, **85**: 064619 (2012)
- 2 J. P. Lestone et al, Nucl. Phys. A, **559**: 277 (1993)
- 3 H. Eslamizadeh Eur. Phys. J. A, **47**: 1 (2011)
- 4 A. Gavron, Phys. Rev. C, **21**: 230 (1980)
- 5 F. Pulnhofer, Nucl. Phys. A, **280**: 267 (1977)
- 6 W. Ye, Int. J. Mod. Phys. E, **23**: 1460003 (2014)
- 7 P. N. Nadtochy et al, Phys. Rev. C, **89**: 014616 (2014)
- 8 H. Eslamizadeh and M. Soltani, Ann. Nucl. Energy, **80**: 261 (2015)
- 9 H. Eslamizadeh, Chinese Phys. C, **39**: 054102 (2015)
- 10 J. P. Lestone and S. G. McCalla, Phys. Rev. C, **79**: 044611 (2009)
- 11 P. N. Nadtochy, G. D. Adeev and A. V. Karpov, Phys. Rev. C, **65**: 064615 (2002)
- 12 H. Eslamizadeh and H. Raanaei, Ann. Nucl. Energy, **51**: 252 (2013)
- 13 P. Fröbrich and I. I. Gontchar, Phys. Rep., **292**: 131 (1998)
- 14 H. Eslamizadeh, Int. J. Mod. Phys. E, **21**: 1 (2012)
- 15 H. Eslamizadeh, Chinese Phys. C, **34**: 1714 (2010)
- 16 W. Ye and N. Wang, Tian J. Phys. Rev. C, **90**: 041604 (2014)
- 17 W. Ye and J. Tian, Phys. Rev. C, **91**: 064603 (2015)
- 18 J. Tian, N. Wang and W. Ye, Chinese Phys. C, **39**: 034102 (2015)
- 19 E. G. Ryabov, A. V. Karpov, P. N. Nadtochy and G. D. Adeev, Phys. Rev. C, **78**: 044614 (2008)
- 20 H. Eslamizadeh and M. Pirpour, Chinese Phys. C, **38**: 064101 (2014)
- 21 J. P. Lestone, Phys. Rev. C, **59**: 1540 (1999)
- 22 N. Wang and W. Ye, Phys. Rev. C, **87**: 051601 (2013)
- 23 M. Brack et al, Rev. Mod. Phys., **44**: 320 (1972)
- 24 A. V. Ignatyuk et al, Yad. Fiz., **21**: 1185 (1975)
- 25 K. T. R. Davies, A. Sierk and J. R. Nix, Phys. Rev. C, **13**: 2385 (1976)
- 26 J. P. Lestone, Phys. Rev. C, **51**: 580 (1995)
- 27 W. D. Myers and W. J. Swiatecki, Nucl. Phys., **81**: 1 (1966)
- 28 W. D. Myers and W. J. Swiatecki, Ark Fys., **36**: 343 (1967)
- 29 J. Blocki et al, Nucl. Phys. A, **545**: 511c (1992)
- 30 G. Chaudhuri, and S. Pal, Phys. Rev. C, **65**: 054612 (2002)
- 31 S. Pal and T. Mukhopadhyay, Phys. Rev. C, **57**: 210 (1998)
- 32 D. V. Vanin et al, Phys. Rev. C, **59**: 2114 (1999)
- 33 M. Blann, Phys. Rev. C, **21**: 1770 (1980)
- 34 J. E. Lynn, *The theory of neutron resonance reactions* (Clarendon: Oxford, 1968), p.325
- 35 S. G. McCalla and J. P. Lestone, Phys. Rev. Lett., **101**: 032702 (2008)
- 36 T. Døssing and J. Randrup, Nucl. Phys. A, **433**: 215 (1985)
- 37 J. Randrup, Nucl. Phys. A, **383**: 468 (1982)
- 38 R. Vandenbosch and J. R. Huizenga, *Nuclear Fission* (Academic: New York, 1973)
- 39 A. Bohr in *Proceedings of the United Nations international conference on the peaceful uses of atomic energy* (United Nations: New York, 1956), **2**: 151
- 40 I. Halpern and V. M. Strutinsky, in *Proceedings of the United Nations international conference on the peaceful uses of atomic energy* (United Nations: Geneva, 1958), **15**: 408
- 41 J. P. Lestone et al, J. Phys. G: Nucl. Part. Phys., **23**: 1349 (1997)
- 42 D. J. Hinde et al, Phys. Rev. C, **45**: 1229 (1992)
- 43 J. O. Newton et al, Nucl. Phys. A, **483**: 126 (1988)
- 44 R. J. Charity et al, Nucl. Phys. A, **457**: 441 (1986)
- 45 B. B. Back et al, Phys. Rev. C, **32**: 195 (1985)
- 46 Z. Liu et al, Phys. Rev. C, **54**: 761 (1996)